# Negative coefficient of normal restitution

Patric Müller, Dominik Krengel, and Thorsten Pöschel
*Institute for Multiscale Simulation, Universität Erlangen-Nürnberg, Nägelsbachstraße 49b, 91052 Erlangen, Germany*
(Received 15 February 2012; published 27 April 2012)

This paper shows that negative coefficients of normal restitution occur inevitably when the interaction force between colliding particles is finite. We derive an explicit criterion showing that for any set of material properties there is *always* a collision geometry leading to negative restitution coefficients. While from a phenomenological point of view, negative coefficients of normal restitution appear rather artificial, this phenomenon is generic and implies an important overlooked limitation of the widely used hard sphere model. The criterion is explicitly applied to two paradigmatic situations: for the linear dashpot model and for viscoelastic particles. In addition, we show that for frictional particles the phenomenon is less pronounced than for smooth spheres.

DOI: 10.1103/PhysRevE.85.041306 PACS number(s): 45.70.−n, 45.50.Tn

## I. INTRODUCTION

Both, kinetic theory of granular matter, based on the Boltzmann equation [1–3], as well as highly efficient event-driven molecular dynamics (eMD) simulation of granular matter [4–6] are based on the hard sphere model of particle collisions. Hard sphere collisions are characterized by $\delta$-shaped interaction forces. Therefore, in a collision the particles instantaneously exchange momentum, while their positions stay invariant. Due to the instantaneous character of the collisions, the dynamics of any *finite* hard sphere system is represented by a sequence of binary collisions (events), leading to the main concept of eMD. As only momentum is transferred during a collision, each event is characterized by only two scalar values: The coefficient of normal restitution $\varepsilon_n$ relating the post- and precollisional normal component of the particles' relative velocity and the corresponding coefficient of tangential restitution for the tangential component. For colliding hard spheres located at $\vec{r}_1$ and $\vec{r}_2$, traveling at velocities $\dot{\vec{r}}_1$ and $\dot{\vec{r}}_2$, the coefficient of normal restitution $\varepsilon_n^{\mathrm{HS}}$ is, thus, defined by

$$(\dot{\vec{r}}_1' - \dot{\vec{r}}_2') \cdot \hat{e}_r^0 = -\varepsilon_n^{\mathrm{HS}} \left(\dot{\vec{r}}_1^{\,0} - \dot{\vec{r}}_2^{\,0}\right) \cdot \hat{e}_r^0, \tag{1}$$

where for each quantity $X$, the symbol $X^0$ denotes the value of $X$ at the beginning of the impact at time $t^0$ and $X'$ is the value at time $t^0 + \tau$, when the collision terminates. Equation (1) addresses hard spheres implying instantaneous collisions, $\tau \to 0$. Note that the unit vector $\hat{e}_r \equiv (\vec{r}_2 - \vec{r}_1)/|\vec{r}_2 - \vec{r}_1|$ remains unchanged during a collision, $\hat{e}_r' = \hat{e}_r^0$, due to the instantaneous character of hard sphere collisions. Therefore, $\hat{e}_r^0$ appears on both sides of Eq. (1). For soft sphere collisions characterized by *finite* interaction forces and contact durations $\tau$, this may be invalid: Oblique impacts may lead to variations of the unit vector $\hat{e}_r' \neq \hat{e}_r^0$. Consequently, for soft spheres the coefficient of normal restitution $\varepsilon_n$ is defined by

$$\left(\dot{\vec{r}}_1' - \dot{\vec{r}}_2'\right) \cdot \hat{e}_r' = -\varepsilon_n \left(\dot{\vec{r}}_1^{\,0} - \dot{\vec{r}}_2^{\,0}\right) \cdot \hat{e}_r^0, \tag{2}$$

which reduces to Eq. (1) in the limit $\tau \to 0$. The variation of the unit vector $\hat{e}_r$ during a collision may be expressed by the angle

$$\varphi' \equiv \cos^{-1}\left(\hat{e}_r^0 \cdot \hat{e}_r'\right). \tag{3}$$

For both, kinetic theory based on the Boltzmann equation as well as eMD, it is essential to assume that $\varphi'$ is negligible. Then, Eq. (1) allows for the computation of the post-collisional particle velocities from the impact velocities, that is, the collision rule needed in eMD simulations and also the Jacobian $\partial(\vec{v}_1, \vec{v}_2)/\partial\left(\vec{v}_1', \vec{v}_2'\right)$ needed for the integration of the Boltzmann equation. It was shown, however, that the assumption $\varphi' \approx 0$ is not always justified [7].

In textbooks, the coefficient of normal restitution is frequently assumed to be a material constant [8], $0 \leqslant \varepsilon_n \leqslant 1$. While from experimental (e.g., [9–13]) and theoretical (e.g., [14–18]) studies it is known that the coefficient of normal restitution depends on the impact velocity or is a fluctuating quantity (e.g., [19]) it was still assumed to not fall below zero.

However, for the case of oblique impacts of nanoclusters it was shown recently [20] that the rotation of the unit vector $\varphi'$ may lead to negative values of the coefficient of normal restitution defined by Eq. (1). This surprising result was attributed to the softness of nanoclusters leading to relatively long contact durations which, in turn, may lead to a significant reorientation of the particles' normal vector during a collision.

While the investigation in [20] refers to nanoclusters colliding at very large impact velocity (1850 m/s), here we show that negative coefficients of normal restitution are a much more general phenomenon. We show that negative values occur inevitably for *any* type of collision whose dynamics is governed by *finite* interaction forces leading to finite duration of contact: For any set of material properties there is *always* a collision geometry leading to negative values of $\varepsilon_n^{\mathrm{HS}}$.

We wish to mention that there are alternative definitions of the coefficient of restitution (e.g., [21–25]), which avoid the problem addressed here. However, only the definition Eq. (1) or (2), respectively, referred to as *Newton's model* [26], allows for the computation of the post-collisional vectorial velocities which are needed for both event-driven simulations and kinetic theory.

In Sec. II we introduce our notation. In Sec. III we derive a general condition for negative coefficients, while in Secs. IV and V we specify our findings to particles which interact via a linear dashpot model and to smooth viscoelastic spheres, respectively. Section VI discusses the role of frictional forces between the colliding particles. Finally, in Sec. VII we summarize our results and present some outlook.

## II. COLLISION OF SMOOTH SPHERES

The collision of a pair of smooth spheres of masses $m_1$ and $m_2$, located at $\vec{r}_1$ and $\vec{r}_2$, is governed by Newton's equation

 

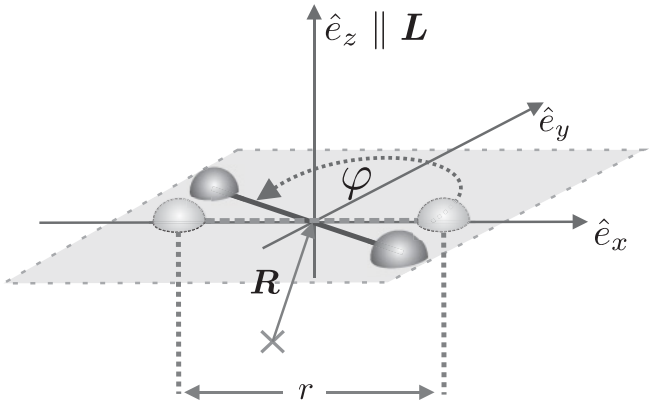


FIG. 1. Geometry of a particle collision.

of motion,

$$m_{\text{eff}}\ddot{\vec{r}} = \vec{F} = F_n \hat{e}_r, \tag{4}$$

where $\vec{r} \equiv \vec{r}_2 - \vec{r}_1$ and $m_{\text{eff}} \equiv m_1 m_2/(m_1 + m_2)$. The collision takes place in a plane perpendicular to the conserved angular momentum

$$\vec{L} = m_{\text{eff}}\, \vec{r} \times \dot{\vec{r}} \equiv L \hat{e}_L. \tag{5}$$

In this collision plane we rewrite Eq. (4) in polar coordinates $\{r,\varphi\}$ (see Fig. 1):

$$m_{\text{eff}}\, r^2 \dot{\varphi} = L, \tag{6a}$$

$$m_{\text{eff}}\, \ddot{r} = F_c + F_n = m_{\text{eff}}\, r\dot{\varphi}^2 + F_n, \tag{6b}$$

with the centrifugal force $F_c$. Together with the initial conditions

$$r(0) = r^0, \quad \dot{r}(0) = \dot{r}^0, \quad \varphi(0) = 0, \tag{7}$$

where we assume that the particles contact at time $t = 0$, Eqs. (6) describe the collision dynamics for an arbitrary normal force $F_n$. The collision terminates at time $t = \tau$ where [18,27]

$$\dot{r}(\tau) > 0 \text{ and } F_n = 0. \tag{8}$$

## III. NEGATIVE VALUES FOR THE COEFFICIENT OF NORMAL RESTITUTION

With the relative vector $\vec{r}$ and its velocity

$$\vec{r} = r\hat{e}_r \quad \text{and} \quad \dot{\vec{r}} = \dot{r}\hat{e}_r + r\dot{\varphi}\hat{e}_\varphi, \tag{9}$$

where

$$\hat{e}_r = \begin{pmatrix} \cos\varphi \\ \sin\varphi \\ 0 \end{pmatrix} \quad \text{and} \quad \hat{e}_\varphi = \begin{pmatrix} -\sin\varphi \\ \cos\varphi \\ 0 \end{pmatrix}, \tag{10}$$

the coefficient of normal restitution [Eq. (1)] reads

$$\varepsilon_n^{\text{HS}} \equiv -\frac{(\dot{r}'\hat{e}'_r + r'\dot{\varphi}'\hat{e}'_\varphi)\cdot\hat{e}^0_r}{(\dot{r}^0\hat{e}^0_r + r^0\dot{\varphi}^0\hat{e}^0_\varphi)\cdot\hat{e}^0_r} = \underbrace{-\frac{\dot{r}'}{\dot{r}^0}}_{>0}\cos\varphi' + \underbrace{\frac{r'\dot{\varphi}'}{\dot{r}^0}}_{\leqslant 0}\sin\varphi'. \tag{11}$$

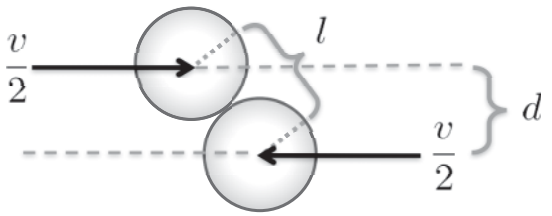


FIG. 2. Eccentric collision of spheres.

To quantify the influence of the post-collisional angle $\varphi'$ on $\varepsilon_n^{\text{HS}}$ we define the function

$$\Delta\varepsilon_n(\varphi') \equiv \frac{\varepsilon_n^{\text{HS}}(\varphi')}{\varepsilon_n^{\text{HS}}(\varphi' = 0)} - 1, \tag{12}$$

such that $\Delta\varepsilon_n < -1$ indicates negative values of $\varepsilon_n^{\text{HS}}$ [see Fig. 4(c)]. Obviously, according to Eqs. (6a) and (7), for this we need two necessary conditions: $L \neq 0$, that is, a noncentral collision and finite contact duration $\tau \neq 0$ which requires a finite interaction force. The second requirement excludes both instantaneous collisions ($\tau \to 0$) which corresponds to $\Delta\varepsilon_n = 0$ and sticky collisions ($\tau \to \infty$) where $\varepsilon_n = 0$ due to vanishing post-collisional velocity.

Let us characterize the eccentricity of the collision by $e \equiv d/l$, see Fig. 2. Then, from geometry and Eq. (5) follows

$$L = m_{\text{eff}}\, v\, d \quad \text{and} \quad \dot{r}^0 = -v\sqrt{1-e^2}. \tag{13}$$

As $L$ is conserved, Eq. (6a) yields

$$r\dot{\varphi} = \frac{v\, d}{r} \tag{14}$$

and the factor in front of the sine term in Eq. (11) reads

$$\frac{r'\dot{\varphi}'}{\dot{r}^0} = -\frac{d}{r'\sqrt{1-e^2}}. \tag{15}$$

Consider *elastic* particles, where $r' = l$[1] and, of course, $\varepsilon_n = 1$ [see Eq. (2)] which implies $\dot{r}^0 = -\dot{r}'$. Then Eq. (11) reads

$$\varepsilon_n^{\text{HS}} = \cos\varphi' - \frac{1}{\sqrt{(1/e)^2 - 1}}\sin\varphi', \tag{16}$$

that is, for fixed impact eccentricity, the value of $\varepsilon_n^{\text{HS}}$ and in particular its sign is governed by the angle $\varphi'$. Figure 3 shows $\varepsilon_n^{\text{HS}}$ for elastic particles as a function of the post-collisional angle $\varphi'$ [Eq. (3)]. We notice two remarkable properties:

(1) Even for elastic particles, $\varepsilon_n^{\text{HS}}$ is not a constant. Besides material properties and impact velocity, it depends on the impact eccentricity and hence on the collision geometry.

(2) Depending on the impact eccentricity, $\varepsilon_n^{\text{HS}}$ may attain negative values for *any* value of $\varphi' \neq 0$.

[1]For inelastic particles this statement would not be correct since the collision terminates before the distance of the particles reaches the sum of the radii, that is, the particles lose contact in slightly compressed state, which has some nontrivial consequences for the coefficient of normal restitution, see [18].

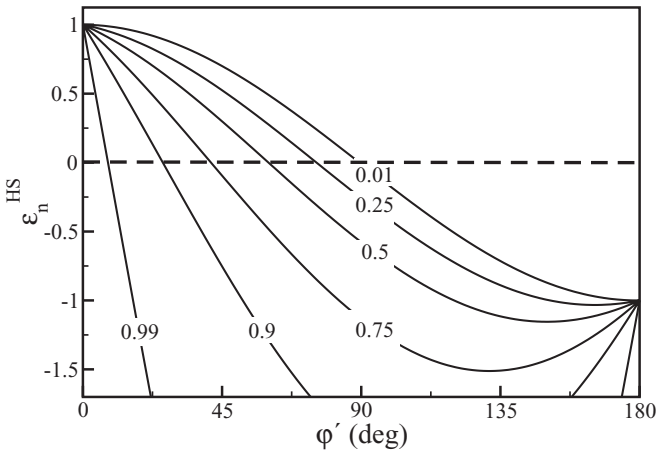


FIG. 3. Coefficient of normal restitution $\varepsilon_n^{\mathrm{HS}}$ [hard sphere definition, Eq. (1)] of elastic particles as a function of the post-collisional angle $\varphi'$ for various impact eccentricities $e \equiv d/l$ [see Eq. (16)].

While colliding, the contacting spheres form a dumbbell-shaped object. For noncentral collisions, $e > 0$, this dumbbell rotates around its center of mass with angular velocity $\dot{\varphi}$ determined by the angular momentum $\vec{L}$ which increases linearly with the impact eccentricity $e$. According to Eq. (6a) this implies that $\dot{\varphi}$ also increases with $e$. For small deformation, $r \approx l$, Eq. (14) yields

$$\dot{\varphi} = \text{const.} = \frac{v\,d}{r^2} \approx e\,\frac{v}{l}. \tag{17}$$

This angular velocity leads to a finite post-collisional rotation angle $\varphi'$ if the duration of the contact is finite, which of course holds for all finite interaction forces. Assuming small deformations, $\varphi'$ is determined by the ratio $\alpha$ of the contact duration $\tau$ and the time $2\pi/\dot{\varphi}$ the dumbbell would need for a full rotation:

$$\alpha \equiv \frac{\tau\dot{\varphi}}{2\pi}, \quad \varphi' = \alpha\,2\pi. \tag{18}$$

For most interaction force laws and realistic material parameters, the post-collisional angle $\varphi'$ is rather small, except for cases where strong attractive forces like adhesion or liquid bridges are involved. Therefore, here we assume $0 \leqslant \varphi' \leqslant \frac{\pi}{2}$ to simplify the notation. In this interval, $\varepsilon_n^{\mathrm{HS}}(\varphi')$ is a monotonously decreasing function for all values of the eccentricity, see Fig. 3. Equation (16) then provides a criterion for negative values of $\varepsilon_n^{\mathrm{HS}}$ for the collision of smooth elastic spheres:

$$\varphi' > \arctan\sqrt{\left(\frac{1}{e}\right)^2 - 1}. \tag{19}$$

With Eq. (18) we obtain

$$\alpha\,2\pi > \arctan\sqrt{\left(\frac{1}{e}\right)^2 - 1} \tag{20}$$

as a criterion to assess whether for a given set of parameters there is a collision geometry leading to negative coefficients of normal restitution.

We emphasize that the value of $\varepsilon_n^{\mathrm{HS}}$ is not related to the dissipative properties of the collision. For the case of elastic collisions shown in Fig. 3, obviously energy is conserved. Nevertheless, except for central collisions (eccentricity $e = 0$), $\varepsilon_n^{\mathrm{HS}}$ adopts values different from unity.

In the following sections we apply these results to two widely used interaction force models. For both models we present exhaustive parameter studies to highlight negative values of $\varepsilon_n^{\mathrm{HS}}$, or more general the geometry dependence of $\varepsilon_n^{\mathrm{HS}}$, as a significant, far reaching effect.

## IV. LINEAR DASHPOT MODEL

The linear dashpot model for the collision of particles defines the interaction force by

$$F_n = k(l - r) - \gamma\dot{r}, \tag{21}$$

see [28]. For a central, elastic collision ($e = 0$, $\gamma = 0$), the duration of contact reads [27]

$$\tau = \pi\sqrt{m_{\mathrm{eff}}/k}, \tag{22}$$

which decays only weakly for moderately off-central collisions, $0 < e \lessapprox 0.8$ [see Fig. 4(a)]. Therefore, due to Eq. (17), $\varphi'$ increases almost linearly with eccentricity [Fig. 4(b)]. Since $-\Delta\varepsilon_n(\varphi')$ increases monotonously for $\varphi' < \pi/2$ [see Eq. (16) and Fig. 3], $\varepsilon_n^{\mathrm{HS}}(e)$ is a decreasing function [Fig. 4(c)].

For larger eccentricity, $e \gtrapprox 0.8$, the centrifugal force dominates the contact mechanics, thus, the contact duration $\tau(e)$ decreases steeply [Fig. 4(a)]. This effect overcompensates the linear growth $\dot{\varphi} \propto e$ [Eq. (17)], turning $\varphi'(e)$ into a decreasing function [Fig. 4(b)].

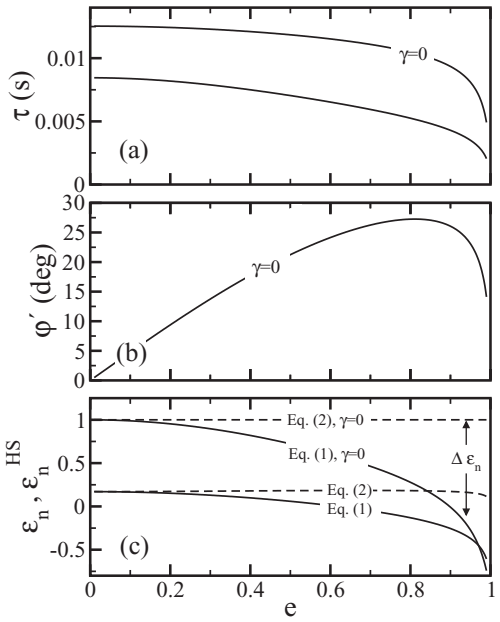


FIG. 4. Linear dashpot model, abscissa of all panels is the impact eccentricity $e \equiv d/l$. (a) Contact duration $\tau(e)$ for the dissipative and the elastic case ($\gamma = 0$). (b) Rotation $\varphi'(e)$ of the normal vector $\hat{e}_r$ at the end of the collision. (c) Coefficient of normal restitution $\varepsilon_n^{\mathrm{HS}}(e)$ due to the hard-sphere definition, Eq. (1) (solid line) and $\varepsilon_n(e)$ due to Eq. (2) (dashed line). Model parameters: $k = 1.5 \times 10^5$ N/m, $R = 0.1$ m, $\rho = 1140$ kg/m$^3$, $v = 10$ m/s, $\gamma = 1000$ kg/s (unless specified otherwise).

Nevertheless, for large eccentricities even small rotation angles $\varphi'$ lead to significant $-\Delta\varepsilon_n(\varphi')$ (see Fig. 3). Consequently, $\varepsilon_n^{\mathrm{HS}}(e)$ is a monotonically decreasing function over the full range of impact eccentricities $e$ [Fig. 4(c), solid line].

Solving Newton's equation, Eqs. (6) with the initial conditions Eq. (7) and the interaction force Eq. (21) together with the condition Eq. (8) for the end of the collision, we obtain the contact duration as a decreasing function of inelasticity $\tau(\gamma)$. Consequently, for all eccentricities $e$, $\varphi'(\gamma)$, and $-\Delta\varepsilon_n(\gamma)$ are decreasing functions. Therefore, for all $e$, the slope of $\varepsilon_n^{\mathrm{HS}}(e)$ for a damped collision is smaller than for the undamped case.

The possibility of intersections of the curves $\varepsilon_n^{\mathrm{HS}}$ for different $\gamma$ [see Fig. 4(c)] may be understood from the fact that both $\varepsilon_n^{\mathrm{HS}}(e=0)$ and $-d\varepsilon_n^{\mathrm{HS}}(e)/de$ decrease with inelasticity.

Using $\tau$ from Eq. (22) and assuming small deformations ($r \approx l$), according to Eq. (18) the rotation angle is approximately given by

$$\varphi' = \alpha\, 2\pi = \pi\, e\frac{v}{l}\sqrt{\frac{m_{\mathrm{eff}}}{k}}. \tag{23}$$

Exploiting the fact that $\varepsilon_n^{\mathrm{HS}}(e)$ decreases with eccentricity and for all eccentricities $-\Delta\varepsilon_n(\varphi')$ is an increasing function, in Figs. 5 and 6 we discuss the parameter dependence of $\varepsilon_n^{\mathrm{HS}}$.

Figure 5(a) shows $\varepsilon_n^{\mathrm{HS}}(e)$ for fixed $k$ but various damping coefficients $\gamma$. It exemplifies the impact of damping detailed in Fig. 4(c). Figure 5(b) displays $\varepsilon_n^{\mathrm{HS}}(e)$ for various spring constants $k$ for elastic particles. As predicted by Eq. (23), $-\Delta\varepsilon_n$ decreases with increasing $k$. Hence the $\varepsilon_n^{\mathrm{HS}}(e)$ curves for larger stiffness $k$ attain larger values for all $e$.

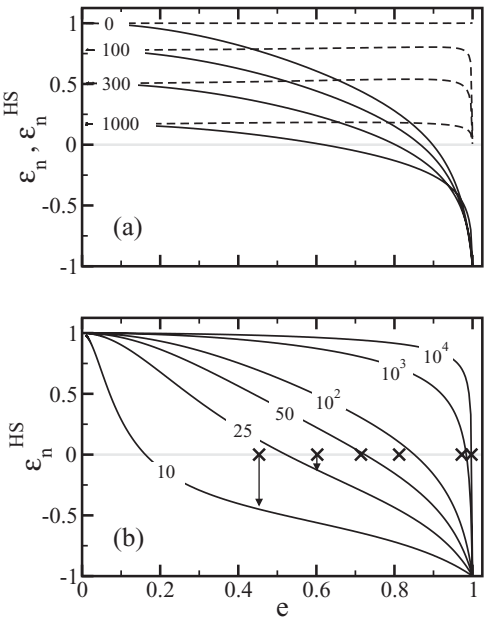


FIG. 5. Linear dashpot model, coefficient of normal restitution vs the impact eccentricity. (a) Solid lines: $\varepsilon_n^{\mathrm{HS}}(e)$ due to Eq. (1), dashed lines: $\varepsilon_n(e)$ due to Eq. (2) for various damping constants $\gamma$ (kg/s). (b) $\varepsilon_n^{\mathrm{HS}}$ for elastic particles ($\gamma = 0$) of various stiffness $k$ (kN/m). Symbols ($\times$) indicate the prediction of Eq. (20) for $\varepsilon_n^{\mathrm{HS}}(e) = 0$. Same parameters as in Fig. 4.

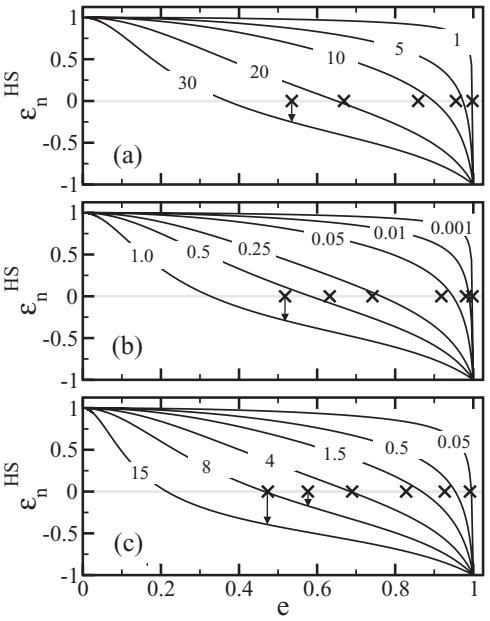


FIG. 6. Linear dashpot model, coefficient of normal restitution as a function of the impact eccentricity $\varepsilon_n^{\mathrm{HS}}(e)$. (a) For various impact velocities $v$ ( m/s); (b) for various particle radii $R$ (m); (c) for various densities $\rho$ ($10^3$ kg/m$^3$). Symbols ($\times$) indicate the theoretical prediction Eq. (20) for $\varepsilon_n^{\mathrm{HS}}(e) = 0$. Same parameters as in Fig. 4.

The same line of reasoning explains Fig. 6: From Eq. (23) we see that $\varphi'$ grows with impact velocity. The $\varepsilon_n^{\mathrm{HS}}(e)$ curves for higher impact velocity hence attain smaller values than those for lower impact velocities [see Fig. 6(a)]. Similarly, the angle $\varphi'(e)$ shows a clear dependence on particle size $R \approx l$ [Fig. 6(b)] and material density $\rho$ ($m_{\mathrm{eff}} \propto \rho$) [see Fig. 6(c)].

The symbols in Figs. 5(b) and 6 indicate the prediction Eq. (20) for the eccentricity where $\varepsilon_n^{\mathrm{HS}}(e)$ changes its sign. As said before, Eq. (20) is a valid approximation for elastic spheres assuming small deformations and impact situations where centrifugal forces can be neglected for the contact duration. It hence fails for small $k$ and $e$ and large $v$, $\rho$, $R$.

## V. VISCOELASTIC SPHERES

As a second important example, we consider the collision of viscoelastic spheres, with the particle-interaction force [16]

$$F_n = F_n^{\mathrm{el}} + F_n^{\mathrm{dis}} = \rho_{\mathrm{el}}(l-r)^{3/2} - \frac{3}{2}A\rho_{\mathrm{el}}\dot{r}\sqrt{l-r}, \tag{24}$$

where

$$\rho_{\mathrm{el}} \equiv \frac{2Y\sqrt{R_{\mathrm{eff}}}}{3(1-\nu^2)} \tag{25}$$

and $Y$, $\nu$, and $R_{\mathrm{eff}}$ denote the Young modulus, the Poisson ratio, and the effective radius $R_{\mathrm{eff}} = R_1R_2/(R_1+R_2)$, respectively. The elastic part $F_n^{\mathrm{el}}$ of this widely used collision model [28–30] is given by the Hertz contact force [31]. The dissipative part $F_n^{\mathrm{dis}}$ was first motivated in [32] and then rigorously derived in [16] and [33], where only the approach in [16] leads to an analytic expression for the parameter $A$, being a function of the elastic and viscous material parameters, see [16] for details.

TABLE I. Elastic characteristics for some common materials [34].

| Material | Young's modulus (GPa) | Density (kg/m$^3$) | Poisson's ratio |
|---|---|---|---|
| Iron | 200 | 7870 | 0.291 |
| Copper | 110 | 8930 | 0.343 |
| Magnesium | 44 | 1740 | 0.35 |
| Nylon | 1 | 1020 | 0.4 |
| Silicon rubber (hard) | 0.1 | 2000 | 0.5 |
| Silicon rubber (soft) | 0.01 | 2000 | 0.5 |

First, we discuss the system behavior for elastic spheres $A = 0$, disregarding dissipation. Figure 7 shows the coefficient of normal restitution $\varepsilon_n^{\rm HS}$ as a function of the impact eccentricity $e$ for some realistic material parameters, see Table I.

From Fig. 7 we notice that the emergence of negative values of $\varepsilon_n^{\rm HS}$ is not restricted to high impact velocity collisions of nanoclusters characterized by strong adhesive forces [20]. Instead, it occurs also for realistic material properties and more realistic impact rate. Moreover, the interval of eccentricity leading to a negative coefficient of restitution is not small, remember that with the assumption of molecular chaos the probability density for a collision with eccentricity $e$ increases linearly, $dp(e)/de \propto e$, $0 \leqslant e < 1$.

Disregarding centrifugal forces, the contact duration reads [18]

$$\tau = 3.218\, R \frac{[\sqrt{2}\pi\rho(1-\nu^2)]^{2/5}}{Y^{2/5}(-\dot{r}^0)^{1/5}}. \tag{26}$$

Assuming small deformations ($r \approx l$), from Eqs. (18) and (13) we find the post-collisional rotation

$$\varphi' = 1.609\, \frac{e}{(\sqrt{1-e^2})^{1/5}}\, v^{4/5} \left[\frac{\sqrt{2}\pi\rho(1-\nu^2)}{Y}\right]^{2/5}. \tag{27}$$

The numerical prefactors in Eqs. (26) and (27) come from a combination of $\Gamma$ functions (see [18,35]).

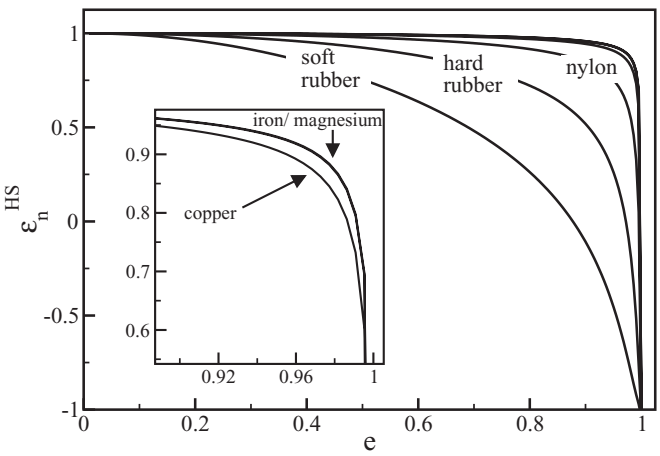


FIG. 7. Elastic spheres (Hertz): coefficient of normal restitution $\varepsilon_n^{\rm HS}$ vs the eccentricity $e$ for some realistic materials. The inset shows a magnification of the main panel. Parameters: $R = 0.1$ m, $v = 10$ m/s and material parameters as specified in Table I.

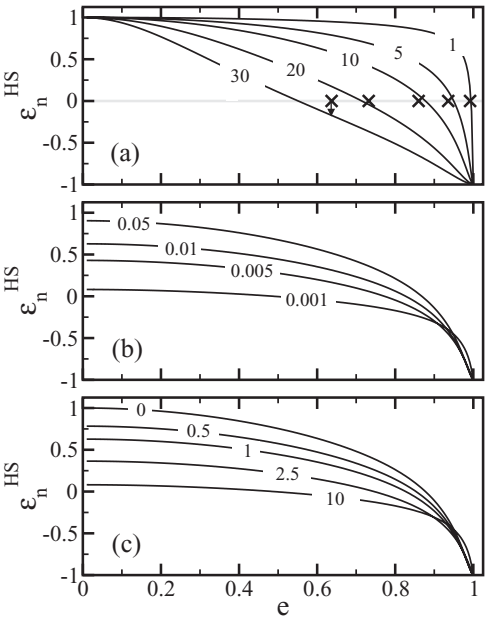


FIG. 8. Viscoelastic spheres, coefficient of normal restitution vs the impact eccentricity $\varepsilon_n^{\rm HS}(e)$ for various values of (a) impact velocity $v$ (m/s) (elastic spheres $A = 0$); (b) particle radius $R$ (m); (c) dissipative constant $A$ ($10^{-3}$ s). Symbols indicate the theoretical prediction [Eq. (20)] for $\varepsilon_n^{\rm HS}(e) = 0$. Model parameters: Soft silicon rubber, see Table I; $R_1 = R_2 = 0.1$ m, $v = 10$ m/s, $A = 10^{-4}$ s (unless specified otherwise).

Following the same line of discussion as in Sec. IV, we obtain again that $\varepsilon_n^{\rm HS}(e)$ is a monotonically decreasing function (see Figs. 7–9). With $\varepsilon_n^{\rm HS}(\varphi')$ [see Eq. (16), Fig. 3] and $\varphi' = \varphi'(e,v,\rho,\nu,Y)$ [see Eq. (27)], we can understand the dependencies of the function $\varepsilon_n^{\rm HS}(e)$ on the material and system parameters, drawn in Figs. 8 and 9.

The influence of the system parameters $R$, $v$, and material characteristics $A$, $\rho$, $Y$ is qualitatively rather similar to the case of particles which interact via a linear dashpot force, described in detail in Sec. IV. Interestingly, for elastic particles Eq. (27) indicates that the rotation angle $\varphi'$ and hence $\varepsilon_n^{\rm HS}$ are independent of the particle radius. For finite inelasticity $A$, however, the dependence on the particle radius enters via $l$ and $\rho_{\rm el}$. Therefore, for inelastic particles, changing radii of the particles has the same impact as changing the inelasticity itself [Fig. 8(b)].

Note that for common materials, the Poisson ratio $\nu$ is of minor importance. Only for highly auxetic materials its influence is not negligible [$\nu \approx -1$, Fig. 9(a)].

The symbols in Figs. 8 and 9 indicate the prediction [Eq. (20)] for the eccentricity where $\varepsilon_n^{\rm HS}(e)$ becomes negative. As stated before, the criterion Eq. (20) is applicable for elastic collisions and to small deformation where, additionally, centrifugal forces may be neglected. If applicable, it yields surprisingly good predictions.

## VI. THE ROLE OF FRICTION

So far we considered the collision of smooth spheres where the interaction force acts in normal direction $\vec{F} = F_n \hat{e}_r$. In this section we address collisions under the action of a repulsive

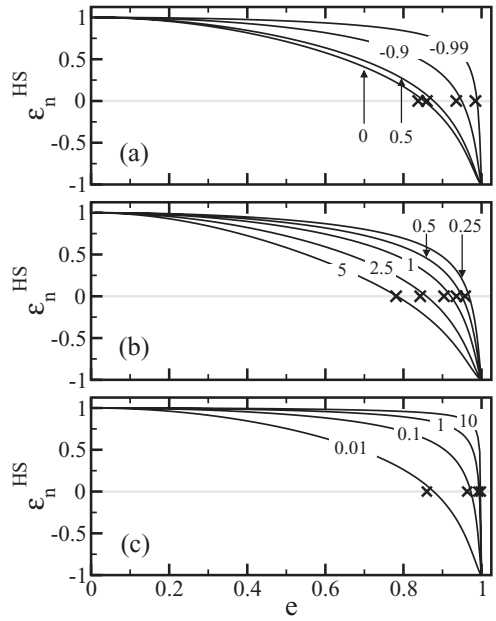


FIG. 9. Elastic spheres ($A = 0$), coefficient of normal restitution as a function of the impact eccentricity $\varepsilon_n^{\mathrm{HS}}(e)$ for various values of (a) Poisson's ratio $\nu$; (b) density $\rho$ ($10^3$ kg/m$^3$); (c) Young's modulus $Y$ (GPa). Symbols indicate the theoretical prediction [Eq. (20)] for $\varepsilon_n^{\mathrm{HS}}(e) = 0$. Same parameters as in Fig. 8.

normal force and an additional friction force acting in tangential direction $\vec{F} = F_n\hat{e}_r + F_t\hat{e}_\varphi$. A tangential force applied to an extended body leads to a torque and, thus, to rotational motion of the particles. For the discussion it is sufficient to consider the collision of particles whose initial angular velocity is zero. With this assumption the collision still takes place in a plane which allows to maintain the notation of Sec. II and the collision geometry sketched in Fig. 2. The rotation of the particles may then be described by scalar quantities $\phi_1$ and $\phi_2$ with the corresponding vectorial representations $\vec{\phi}_1 = \phi_1\,\hat{e}_\phi$ and $\vec{\phi}_2 = \phi_2\,\hat{e}_\phi$. Likewise the angular velocities $\dot{\phi}_1$ and $\dot{\phi}_2$. The equations of motion for the collision then read

$$\begin{aligned} \ddot{r} &= r\dot{\varphi}^2 + \frac{F_n}{m_{\mathrm{eff}}}, \\ \ddot{\varphi} &= -2\frac{\dot{r}\dot{\varphi}}{r} + \frac{F_t}{r\,m_{\mathrm{eff}}}, \\ \ddot{\phi}_1 &= -\frac{1}{I_1}R_1F_t, \quad \ddot{\phi}_2 = \frac{1}{I_2}R_2F_t, \end{aligned} \tag{28}$$

where $I_1 = \frac{2m_1R_1^2}{5}$ and $I_2 = \frac{2m_2R_2^2}{5}$ are the moments of inertia of the spheres. The initial conditions are

$$\begin{aligned} &r(0) = r^0; \quad \dot{r}(0) = \dot{r}^0; \quad \varphi(0) = 0; \quad \dot{\varphi}(0) = \dot{\varphi}^0 = e\frac{v}{l}; \\ &\phi_1(0) = 0; \quad \phi_2(0) = 0; \quad \dot{\phi}_1(0) = 0; \quad \dot{\phi}_2(0) = 0. \end{aligned} \tag{29}$$

Let us assume a large enough friction $\mu \to \infty$ such that the colliding particles do not slide on one another but form a dumbbell for the duration of the collision, that is, the particles rotate together with the dumbbell. Its moment of inertia with respect to an axis through its center of mass, perpendicular to its axis of symmetry, reads $I_{\mathrm{fric}} = \frac{14mR^2}{5}$ if we further assume identical particles. In contrast, for smooth spheres (i.e., $\dot{\phi}_1 = \dot{\phi}_2 = 0$) the corresponding moment of inertia of the dumbbell is given by $I_{\mathrm{smooth}} = 2mR^2$. From conservation of angular momentum (consisting of orbital angular momentum of the two particles and the particle spin) we obtain the ratio of the rotation velocity of the dumbbell for the cases of smooth and frictional spheres:

$$\frac{\dot{\varphi}^0_{\mathrm{fric}}}{\dot{\varphi}^0_{\mathrm{smooth}}} = \frac{I_{\mathrm{smooth}}}{I_{\mathrm{fric}}} = \frac{10}{14} \approx 0.71. \tag{30}$$

Since the contact duration is only weakly affected by friction, from Eq. (30) follows that for frictional particles the rotation angle of the unit vector is reduced as compared with the nonfrictional case $\varphi'_{\mathrm{fric}} \approx 0.71\,\varphi'_{\mathrm{smooth}}$. Consequently, for all eccentricities $-\Delta\varepsilon_n(e)$ is smaller for frictional than for smooth particles and, thus, the function $\varepsilon_n^{\mathrm{HS}}(e)$ attains higher values for frictional than for smooth particles. Therefore, friction reduces the decay of the function $\varepsilon_n^{\mathrm{HS}}(e)$ and the effect of negative coefficients of normal restitution is shifted toward larger values of $e$ (see Fig. 10).

For illustration we specify the tangential force to the widely used model by Cundall and Strack [36]:

$$F_t = -\mathrm{sign}\,\zeta(t)\cdot\min(k^t|\zeta|, \mu|m_{\mathrm{eff}}r\dot{\varphi}^2 + F_n|), \tag{31}$$

where

$$\zeta(t) = \int_{t'=0}^{t} v_{\mathrm{rel,t}}(t')dt', \tag{32}$$

$$v_{\mathrm{rel,t}} = r\dot{\varphi} + (R_2\dot{\phi}_2 - R_1\dot{\phi}_1), \tag{33}$$

and $k^t$ and $\mu$ are the stiffness of the contact and the friction parameter, respectively. Figure 10 displays the influence of friction on the coefficient of restitution $\varepsilon_n^{\mathrm{HS}}(e)$ for both normal force models, the linear dashpot [Fig. 10(a)] and for viscoelastic spheres [Fig. 10(b)]. As described above, in both cases friction partially suppresses the rotation angle of the unit

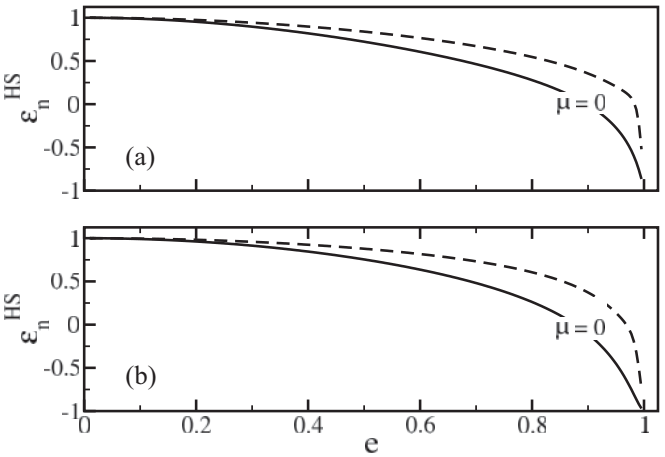


FIG. 10. Elastic frictional spheres, coefficient of normal restitution vs the impact eccentricity $\varepsilon_n^{\mathrm{HS}}(e)$ (dashed lines, $\mu \neq 0$) and smooth spheres (solid lines, $\mu = 0$). (a) Linear dashpot model, same parameters as in Fig. 4; (b) Hertz force, same parameters as in Fig. 8. Parameters of the friction force: $k^t = 10^5$ N/m, $\mu = 10^8$.

vector $\varphi'$. Therefore, for frictional particles, $-\Delta\varepsilon_n$ is smaller than for smooth spheres.

## VII. SUMMARY

The concept of the coefficient of restitution, characterizing the mechanics of binary collisions of granular particles is the foundation of both, highly efficient event-driven molecular dynamics simulations and kinetic theory of granular gases and rapid granular flows. Obviously the underlying assumption of instantaneous collisions is an idealization which is not in strict agreement with the dissipative nature of particle collisions. Indeed, for any realistic material, the elastic and dissipative interaction forces are finite enforcing a finite duration of collisions.

The detailed consideration of the interaction forces leads to two conclusions: First, the coefficient of restitution is not a material constant but depends on the impact rate. This experimentally known fact (e.g. [10]) agrees with theoretical results based on the numerical [16] or analytical [17,18,27,35] solution of Newton's equation of motion for the collision process. Second, in contrast to the assumption of instantaneous collisions, the intercenter unit vectors of the particles $\hat{e}_r$ just before and just after the collision are not identical (e.g. [7]) except for perfectly central collisions. While the first result was taken into account for simulations and kinetic theory by many authors, so far the rotation of the unit vector is disregarded for eMD and kinetic theory. With the most natural assumption of molecular chaos in granular gases and rapid granular flows, the majority of collisions is, however, not close to central but rather eccentric due to the probability distribution $dp(e) \propto e\,de$ for the eccentricity $0 \leqslant e < 1$ (see Fig. 2). It may, hence, be questioned whether the concept of the coefficients of restitution is justified.

In a recent paper by Saitoh *et al.* [20] it was shown that the oblique collision of highly adhesive clusters of nanoparticles at very large impact rate leads not only to the expected dependence of $\varepsilon_n$ on the impact rate but also on the impact geometry, namely on the eccentricity $e$ which may lead even to negative values of $\varepsilon_n$ when the common hard-sphere definition Eq. (1) is applied. Inspired by [20], in this paper we focus on the simplest case, namely the coefficient of normal restitution $\varepsilon_n$ for colliding soft and frictional spheres. In particular, we raise the question whether the coefficient of normal restitution is always positive.

In this work we show that both the dependency of the coefficient of normal restitution on the impact geometry as well as negative values of the coefficient are not a peculiarity of colliding nanoclusters. In opposite we show that the described effects are unavoidable for all kind of collisions governed by finite interaction forces. We specify our results to two important interaction forces, the linear-dashpot force and the force between viscoelastic spheres. The former is of importance for kinetic theory as it leads for central collisions $e = 0$ to an impact-velocity independent coefficient of normal restitution, which is widely used in the literature on granular gases and rapid granular flows. The latter leads for $e = 0$ to an impact-velocity dependent coefficient of restitution which is inconvenient for kinetic theory but important for realistic simulations of granular systems.

For both cases we study the effect of impact eccentricity on the coefficient of normal restitution for a wide range of realistic material and system parameters. We find that the emergence of negative values of the coefficient of normal restitution is not restricted to collisions of nanoclusters characterized by strong adhesive forces at high impact velocity [20], but it is a significant effect for particles of common materials under rather common conditions. Consequently, the dependence of $\varepsilon_n$ on the impact geometry should be taken into account for the kinetic theory of granular systems. Since unavoidable negative values of $\varepsilon_n$ render highly efficient event-driven MD impossible, we believe that new approaches should be developed for event-driven simulations which is subject of ongoing research.

## ACKNOWLEDGMENTS

The authors gratefully acknowledge the support of the Cluster of Excellence 'Engineering of Advanced Materials' at the University of Erlangen-Nuremberg, which is funded by the German Research Foundation (DFG) within the framework of its 'Excellence Initiative.'

[1] I. Goldhirsch, Annu. Rev. Fluid Mech. **35**, 267 (2003).
[2] N. V. Brilliantov and T. Pöschel, *Kinetic Theory of Granular Gases* (Oxford University Press, Oxford, 2010).
[3] T. Pöschel and N. Brilliantov, Eds., *Granular Gas Dynamics*, Lecture Notes in Physics (Springer, Berlin, 2003).
[4] B. D. Lubachevsky, J. Comput. Phys. **94**, 255 (1991).
[5] D. C. Rapaport, J. Comput. Phys. **34**, 184 (1980).
[6] T. Pöschel and T. Schwager, *Computational Granular Dynamics* (Springer, Berlin, 2005).
[7] V. Becker, T. Schwager, and T. Pöschel, Phys. Rev. E **77**, 011304 (2008), Fig. 12.
[8] S. T. Thornton and J. B. Marion, *Classical Dynamics of Particles and Systems* (Brooks/Cole, Belmont, MA, 2004), p. 359.
[9] C. V. Raman, Phys. Rev. **12**, 442 (1918).
[10] F. G. Bridges, A. Hatzes, and D. N. C. Lin, Nature (London) **309**, 333 (1984).
[11] S. Wall, W. John, H.-C. Wang, and S. L. Goren, Aerosol Sci. Technol. **12**, 926 (1990).
[12] S. F. Foerster, M. Y. Louge, H. Chang, and K. Allia, Phys. Fluids **6**, 1108 (1994).
[13] P. F. Luckham, Powder Technol. **58**, 75 (1989).
[14] W. Goldsmith, *Impact: The Theory and Physical Behaviour of Colliding Solids* (Edward Arnold, London, 1960).
[15] R. M. Brach, J. Appl. Mech. **56**, 133 (1989).
[16] N. V. Brilliantov, F. Spahn, J.-M. Hertzsch, and T. Pöschel, Phys. Rev. E **53**, 5382 (1996).
[17] T. Schwager and T. Pöschel, Phys. Rev. E **57**, 650 (1998).
[18] T. Schwager and T. Pöschel, Phys. Rev. E **78**, 051304 (2008)

[19] M. Montaine, M. Heckel, C. Kruelle, T. Schwager, and T. Pöschel, Phys. Rev. E **84**, 041306 (2011).
[20] K. Saitoh, A. Bodrova, H. Hayakawa, and N. V. Brilliantov, Phys. Rev. Lett. **105**, 238001 (2010).
[21] W. J. Stronge, Proc. R. Soc. London Ser. A **431**, 169 (1990).
[22] W. J. Stronge, Int. J. Impact Eng. **15**, 435 (1994).
[23] C. E. Smith and P.-P. Liu, J. Appl. Mech. **59**, 963 (1992).
[24] C. E. Smith, J. Appl. Mech. **58**, 754 (1991).
[25] Y. Wang and M. T. Mason, J. Appl. Mech. **59**, 635 (1992).
[26] G. Gilardi and I. Sharf, Mech. Machine Theory **37**, 1213 (2002).
[27] T. Schwager and T. Pöschel, Granular Matter **9**, 465 (2007).
[28] J. Schäfer, S. Dippel, and D. E. Wolf, J. Phys. I (France) **6**, 5 (1996).
[29] H. Kruggel-Emden, E. Simek, S. Rickelt, S. Wirtz, and V. Scherer, Powder Technol. **171**, 157 (2007).
[30] A. B. Stevens and C. M. Hrenya, Powder Technol. **154**, 99 (2005).
[31] H. Hertz, J. Reine Angewandte Mathematik **92**, 156 (1882).
[32] G. Kuwabara and K. Kono, Jpn. J. Appl. Phys. **26**, 1230 (1987).
[33] W. A. M. Morgado and I. Oppenheim, Phys. Rev. E **55**, 1940 (1997).
[34] MatWeb, online resource, accessed March 2012, http://www.matweb.com/
[35] R. Ramírez, T. Pöschel, N. V. Brilliantov, and T. Schwager, Phys. Rev. E **60**, 4465 (1999).
[36] P. A. Cundall and O. D. L. Strack, Géotechnique **29**, 47 (1979).